

# Secretome of the Biocontrol Agent *Metarhizium anisopliae* Induced by the Cuticle of the Cotton Pest *Dysdercus peruvianus* Reveals New Insights into Infection

Walter O. Beys-da-Silva,<sup>\*,†</sup> Lucélia Santi,<sup>†</sup> Markus Berger,<sup>§</sup> Diego Calzolari,<sup>†</sup> Dario O. Passos,<sup>‡</sup> Jorge A. Guimarães,<sup>§</sup> James J. Moresco,<sup>†</sup> and John R. Yates<sup>†</sup>

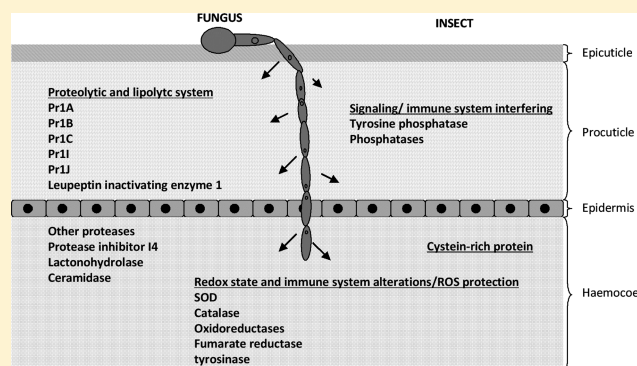
<sup>†</sup>Department of Chemical Physiology and <sup>‡</sup>Department of Cell and Molecular Biology, The Scripps Research Institute, 10550 North Torrey Pines Road, La Jolla, California 92037, United States

<sup>§</sup>Centro de Biotecnologia, Universidade Federal do Rio Grande do Sul, Av. Bento Gonçalves, 9500, P.O. Box 15001, 91501-970 Porto Alegre, RS, Brazil

## S Supporting Information

**ABSTRACT:** *Metarhizium anisopliae* is an entomopathogenic fungus that has evolved specialized strategies to infect insect hosts. Here we analyzed secreted proteins related to *Dysdercus peruvianus* infection. Using shotgun proteomics, abundance changes in 71 proteins were identified after exposure to host cuticle. Among these proteins were classical fungal effectors secreted by pathogens to degrade physical barriers and alter host physiology. These include lipolytic enzymes, Pr1A, B, C, I, and J proteases, ROS-related proteins, oxidoreductases, and signaling proteins. Protein interaction networks were generated postulating interesting candidates for further studies, including Pr1C, based on possible functional interactions. On the basis of these results, we propose that *M. anisopliae* is degrading host components and actively secreting proteins to manage the physiology of the host. Interestingly, the secretion of these factors occurs in the absence of a host response. The findings presented here are an important step in understanding the host–pathogen interaction and developing more efficient biocontrol of *D. peruvianus* by *M. anisopliae*.

**KEYWORDS:** *Metarhizium anisopliae*, shotgun proteomics, biocontrol, host infection, *Dysdercus peruvianus*



## INTRODUCTION

Among the several types of biocontrol agents, the pathogenic arthropod microorganisms such as the filamentous fungus *Metarhizium anisopliae* deserve special attention. This fungus can infect a broad range of arachnid and insect hosts, from agricultural pests to vectors of human disease and recently the venomous spider *Loxosceles* sp.<sup>1–4</sup> *M. anisopliae* is also one of the most studied and applied biological control agents worldwide.<sup>2</sup> This fungus has been successfully applied since the 1970s in Brazil to control sugar cane pests, but the slow speed to kill some targets compared with chemical pesticides limits its commercial adoption. Understanding the molecular mechanisms of the host/fungus interaction and identifying the proteins specifically expressed during the infection are crucial steps to improve biocontrol. The information can be applied to optimize commercial formulations or identify more efficient strains in nature or in fungal libraries.

Crop losses in Brazil caused by arthropods can reach 75% for upland cotton and 35% for perennial cotton, of which about half is caused specifically by cotton stainer bugs (*Dysdercus* spp., Hemiptera: Pyrrhocoridae).<sup>4,5</sup> *Dysdercus peruvianus* causes

damage by eating cotton seed, staining the fibers, and transmitting phytopathogenic bacteria and fungi.<sup>4</sup>

The host-infection process of *M. anisopliae* begins with conidial adhesion to the host's exoskeleton surface (unlike other biocontrol agents that require ingestion). After that, proteins are secreted for cuticle penetration and the enzyme activities that are secreted depend on the cuticle composition of the host.<sup>1</sup> Digestion of the cuticle is multifactorial and involves the mechanical pressure of the host tegument by apressorium combined with the participation of secreted hydrolytic and degradative enzymes, like proteases, chitinases, and lipases, that allow the penetration of the fungi through the host cuticle.<sup>1,6–9</sup> During these events, classical aspects of the host immune system are activated, triggering countermeasures to the invading fungus. The dynamic interaction between fungus and insect is poorly defined but consists of both shared and species-specific components. The discovery of the insect-specific components may enable the development of improved formulations of biocontrol agents.

**Received:** October 17, 2013

**Published:** April 7, 2014

The fungal proteins secreted during the interaction of *M. anisopliae* and *D. peruvianus* have not been analyzed in depth. Two proteins (GAPDH and phosphatase) have been implicated in the first step of infection and adhesion.<sup>10,11</sup> An initial attempt to globally analyze this system identified only eight proteins.<sup>12</sup> The mechanism of *M. anisopliae* infection of the cotton stainer bug is unclear, and new studies are needed to better elucidate the mechanisms involved in invasion.

In this work, we used insect cuticle to activate the fungal infection system<sup>12</sup> and analyzed the secreted proteins by shotgun proteomics. We identified proteins previously reported and also several new proteins for this system. Differentially secreted proteins were also analyzed in silico, producing a network that revealed the potential interaction among proteins identified. The proteomic results were validated through selected enzymatic assays. The results present in this article are an important contribution to an understanding of this host–pathogen system.

## MATERIALS AND METHODS

### Culture Conditions and Cuticle Preparation

*M. anisopliae* var. *anisopliae* E6 (ITS-based species identification GenBank Accession Number EF051705) isolated from spittlebug (*Deois flavopicta*) from the state of Espírito Santo, Brazil was kept in Cove's medium, and conidia were produced for liquid culture growth, as previously described.<sup>13</sup> Spores ( $10^7$  mL<sup>-1</sup>) were inoculated in 70 mL of basal medium (BM; 0.6% NaNO<sub>3</sub>, 0.2% glucose, 0.2% peptone, 0.05% yeast extract) containing 0.05% cholesteryl stearate and 0.7% *D. peruvianus* (DP) cuticle (as infection condition) or 1% glucose (G) for the control condition to mimic infection conditions.<sup>7</sup> The flasks were incubated at 28 °C with shaking (150 rpm) for 48 or 96 h. The choice for this culture medium and culture times and conditions was made based on our previous work,<sup>7</sup> where we detected infection enzymes, lipases, and proteases differentially in the presence of host cuticle components compared with different controls, where one of them was 1% glucose. Also, in this previous work, we have proved that glucose had no influence on the secretion of these enzymes. Therefore, glucose is not acting as a catabolite repressor and can be used to define the constitutive secretome, as previously used.<sup>14–19</sup> A more detailed discussion about the use of glucose as control condition is presented as Supporting Information S1.

For cuticle preparation, adults of *D. peruvianus* were crushed by pressing and centrifuged 10 min, 8,000g, to remove internal material. The cuticles were rinsed extensively five times with sterile, distilled water and sterilized by autoclaving and dried at 50 °C before use in liquid cultures.

After growth, 0.25% (v/v) Triton X-100 was added and manually mixed to extract enzymes and proteins from the external surface, as previously described.<sup>13</sup> Mycelia were harvested by filtration through a Whatman no. one filter paper. These culture filtrates containing secreted proteins were used for experiments. After the filtration, 65 mL of each culture sample was immediately boiled for 15 min to inactivate *M. anisopliae* proteases, followed by freezing at –80 °C and lyophilization. Five mL of each replicate was directly frozen in 200 µL aliquots and kept at –80 °C for enzymatic assays.

### Rearing of *Dysdercus peruvianus*

The insects used in this work were kindly provided by Dr. Célia Carlini from Departamento de Biofísica of Universidade Federal do Rio Grande do Sul. In brief, colonies of *D. peruvianus* were maintained in transparent plastic flasks covered with a screen.

Insects were provided with cotton seeds (*Gossypium hirsutum*) as a food source and sterile water.<sup>4</sup> Colonies of adult insects were maintained in a humid chamber (>90% RH) at 28 °C with a 16L:8D photoperiod.

### Bioassays

Three groups of 20 adult insects were chosen randomly and used in each experiment. For exposure, insects were totally immersed in a suspension of  $10^8$  *M. anisopliae* conidia mL<sup>-1</sup> for 15 s. After immersion, insects were separated into three groups of 20 (60 for each treatment) and placed in glass flasks (63 cm<sup>2</sup> × 12 cm) covered with a screen tissue and provided with cotton seeds and sterile water. All groups were maintained in a humidity chamber (90% RH) at 28 °C under a 16:8 L:D photoperiod. Insects were observed daily to determine survival and mortality. Individual experiments were replicated three times. As a control, insects were treated in exactly the same way, but they were immersed in sterile water instead of the conidial suspension.

Protein measurements were carried out using the bicinchoninic acid (BCA) protein assay (Pierce, Rockford, IL) with bovine serum albumin as the standard.<sup>20</sup>

### Preparation of Protein Extracts

Lyophilized supernatants were resuspended in small volumes of purified water (JTBaker, USA) and precipitated using methanol/chloroform. After precipitation, samples were dried at 37 °C and resuspended in water. The protein concentration was determined using the BCA assay (Thermo Scientific, IL).

### Sample Preparation for Mass Spectrometry

Approximately 100 µg *M. anisopliae* secreted proteins in DP cuticle or glucose (48 and 96h) was suspended in digestion buffer (8 M urea, 100 mM tris-HCl pH 8.5). Proteins were reduced with 5 mM tris-2-carboxyethyl-phosphine (TCEP) at room temperature for 20 min and alkylated with 10 mM iodoacetamide at room temperature in the dark for 15 min. After the addition of 1 mM CaCl<sub>2</sub> (final concentration), the proteins were digested with 2 µg of trypsin (Promega, Madison, WI) by incubation at 37 °C during 16 h. Proteolysis was stopped by adding formic acid to a final concentration of 5%. Samples were centrifuged at 14 000 rpm for 20 min, and the supernatant was collected and stored at –80 °C. Three biological replicates and two technical replicates were analyzed for both *M. anisopliae* culture conditions (48 or 96 h in DP and G).

### MudPIT

The protein digest was pressure-loaded into a 250 µm i.d. capillary packed with 2.5 cm of 5 µm Luna strong cation exchanger (SCX) (Whatman, Clifton, NJ) followed by 2 cm of 3 µm Aqua C18 reversed-phase (RP) (Phenomenex, Ventura, CA) with a 1 µm frit. The column was washed with buffer containing 95% water, 5% acetonitrile, and 0.1% formic acid. After washing, a 100 µm i.d. capillary with a 5 µm pulled tip packed with 11 cm of 3 µm Aqua C18 resin (Phenomenex, Ventura, CA) was attached via a union. The entire split-column was placed in line with an Agilent 1100 quaternary HPLC (Palo Alto, CA) and analyzed using a modified 12-step separation, as previously described.<sup>21</sup> The buffer solutions used were 5% acetonitrile/0.1% formic acid (Buffer A), 80% acetonitrile/0.1% formic acid (Buffer B), and 500 mM ammonium acetate, 5% acetonitrile, and 0.1% formic acid (Buffer C). Step 1 consisted of a 70 min gradient from 0–100% (v/v) buffer B. Steps 2–10 had a similar profile with the following changes: 3 min in 100% (v/v) buffer A, 3 min in X% (v/v) buffer C, 4 min gradient from 0 to 10% (v/v) buffer B, and 101 min gradient from 10–100% (v/v)

buffer B. The 3 min buffer C percentages (X) were 10, 20, 30, 40, 50, 60, 70, 80, 90, and 100% (v/v). An additional step containing 3 min in 100% (v/v) buffer A, 3 min in 90% (v/v) buffer C and 10% (v/v) buffer B, and 110 min gradient from 10–100% (v/v) buffer B were used.

### Linear Trap Quadrupole Ion Trap

Peptides eluted from the microcapillary column were electrosprayed directly into an LTQ-XL mass spectrometer (Thermo Finnigan, Palo Alto, CA) with the application of a distal 2.4 kV spray voltage. A cycle of one full-scan mass spectrum (300–2000 *m/z*) followed by five data-dependent MS/MS spectra at a 35% normalized collision energy was repeated continuously throughout each step of the multidimensional separation. To prevent repetitive analysis, dynamic exclusion was enabled with a repeat count of 1, a repeat duration of 30 s, and an exclusion list size of 200. Application of mass spectrometer scan functions and HPLC solvent gradients was controlled by the Xcalibur data system (Thermo, San Jose, CA).

### Analysis of Tandem Mass Spectra

Tandem mass spectra were analyzed using the following software analysis protocol. Protein identification and quantification analysis were done with Integrated Proteomics Pipeline (IP2, Integrated Proteomics Applications, Inc., [www.integratedproteomics.com/](http://www.integratedproteomics.com/)). Tandem mass spectra were extracted into ms2 files from raw files using RawExtract 1.9.9<sup>22</sup> and were searched using ProLuCID algorithm<sup>23</sup> against the *M. anisopliae* ARSEF23 database from the National Center for Biotechnology Information (NCBI) (<http://www.ncbi.nlm.nih.gov/genome/?term=metarhizium%20anisopliae%20arsef23>, downloaded on August 8, 2012). The peptide mass search tolerance was set to 3 Da, and carboxymethylation (+57.02146 Da) of cysteine was considered to be a static modification. ProLuCID results were assembled and filtered using the DTASelect program<sup>24</sup> using two SEQUEST<sup>25</sup>-defined parameters: the cross-correlation score (XCORR) and normalized difference in cross-correlation scores (DeltaCN) to achieve a false discovery rate of 1%. The following parameters were used to filter the peptide candidates: -p 1 -y 1 --trypstat --fpf 0.01 --dm -in.

### Data Analysis

The software PatternLab<sup>26,27</sup> was used to identify differentially expressed proteins (TFold module)<sup>28</sup> found in 48 and 96 h of *M. anisopliae* grown in DP cuticle. Spectral counting (as used by PatternLab) is a well-established semiquantitative method of determining relative protein abundance.<sup>29</sup> The following parameters were used: proteins that were not detected in at least four out of six runs per condition were not considered, and BH *q* value of 0.05 (5% FDR) was set. Each individual protein was calculated according to the *t* test (*p* value of 0.005) using an F stringency of 0.04. Also, an absolute fold change greater than two was used to select differentially expressed proteins. PatternLab's Approximate Area Proportional Venn Diagram (AAPVD) module was used for pinpointing exclusive proteins identified in a condition using a probability of 0.01.

The Blast2GO tool (<http://www.blast2go.org>)<sup>30</sup> was used to categorize the proteins detected by Gene Ontology (<http://www.geneontology.org>) (GO) annotation<sup>31</sup> according to biological process and molecular function.

Other bioinformatic tools were used to investigate the characteristics of those proteins identified by MudPIT. The TargetP 1.0 (cutoff >0.9),<sup>32</sup> TMHMM 2.0, and Wolf PSORT<sup>33</sup> (<http://wolfsort.seq.cbrc.jp/>) were used to evaluate the subcellular

location, and SignalP 4.1<sup>34</sup> and PredGPI<sup>35</sup> (<http://gpcr.biocomp.unibo.it/predgpi/index.htm>) were used for prediction of secreted proteins. TargetP, TMHMM, and SignalP programs are available in <http://www.cbs.dtu.dk/services/>. To avoid false-positives, we made the following analysis: (1) All proteins identified as secreted using TargetP and SignalP were extracted and then ran using TMHMM. (2) Simultaneously, the PredGPI program was applied. Then, all positive proteins yielded from steps (1) and (2) were used as input for WolfPSORT to discard false-positives. One protein was considered secreted if it was positive in all of these programs: steps (1) plus (2) and WolfPSORT. At the same time, we also used the program SECRETOOL<sup>36</sup> as alternative analysis.

We also ran an analysis of the *M. anisopliae* secretome using the OrthoMCL program<sup>37</sup> (<http://orthomcl.org/orthomcl/>) to get valid assignments of our identified proteins to OrthoMCL-DB groups, a set of proteins across one or more species that represent putative orthologs and in-paralogs.<sup>37</sup>

### Interaction Data Set

To construct a reference data set with the known interactions for the *M. anisopliae*, starting from the protein regulation data set originated from PatternLab's AAPV module, we downloaded from Uniprot (<http://www.uniprot.org>) the database release uniprot\_sprot\_fungi\_01\_13. We developed an in-house software tool to parse the protein list to extract the Gene Ontology terms. For every possible protein pair, an "ontological distance" was calculated considering the fraction of GO terms shared over the sum of all distinct terms; the resulting score is then bounded between 0 and 1.

### Network Maps and Visualization

We developed an in-house software tool to parse the protein ontological distance list into an interaction network. Each interaction is not directional and is representative of the corresponding score in the ontological distance data set. Each node in the interactions list is assigned a color based on its value in the protein regulation data set ranging in a gradient from blue, for down-regulated values, to red, for up-regulated ones. To visualize the network we used the open source Medusa viewer.<sup>38</sup>

More detailed information about the interaction network is presented as Supporting Information S2.

### Validation

For the protease assays, chromogenic substrates were used as previously described.<sup>8</sup> Ten microliters of samples was incubated in 20 mM Tris–HCl buffer, pH 7.4. The reactions were initiated by adding DL-BAPNA (benzoyl-DL-arginine- $\rho$ NA) or Pr1-specific synthetic peptide substrate (Suc-ala-ala-pro-phe- $\rho$ NA) at 0.2 mM (final concentration). Kinetic assays were monitored at 37 °C for 30 min in a SpectraMax spectrophotometer equipped with thermostat and shaking systems. One protease unit (U) was defined as the amount of enzyme that produces one  $\mu$ mol of  $\rho$ -nitroaniline per hour under the assay conditions described.

The catalase activity was assayed using hydrogen peroxide as substrate.<sup>8</sup> Phosphate buffer was added along with H<sub>2</sub>O<sub>2</sub> 10 mM to 25 mL sample aliquots. Catalase activity was estimated by the decrease in absorbance of H<sub>2</sub>O<sub>2</sub> at 240 nm for 3 min. The decomposition of H<sub>2</sub>O<sub>2</sub> was followed at 240 nm ( $E = 39.4 \text{ mm cm}^{-1}$ ).

The assay for superoxide dismutase (SOD) was conducted as previously described.<sup>8</sup> A solution containing 0.05 M potassium phosphate buffer pH 7.8, 13 mM L-methionine, 75 mM NBT (nitrobluetetrazolium), 0.1 mM EDTA, and 0.025% Triton X-100 was added to glass tubes. To start the reactions, we added



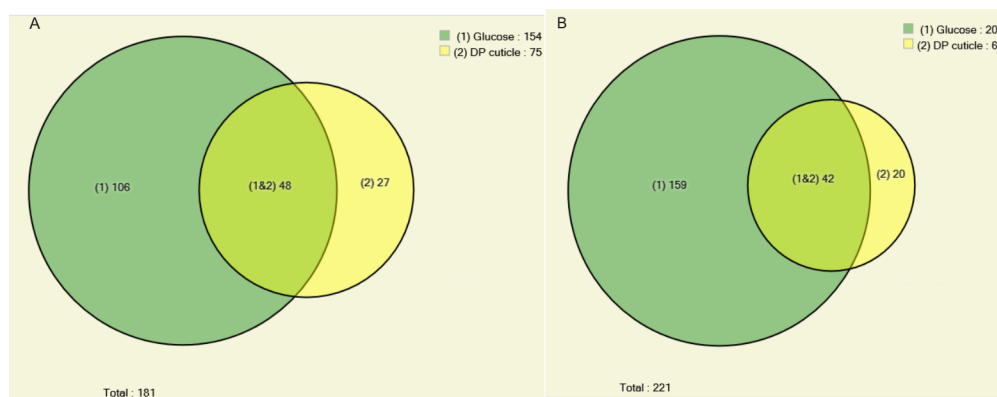


**Figure 1.** Distribution and overlap of proteins from *M. anisopliae* supernatant when grown in *D. peruvianus* cuticle medium after (A) 48 or (B) 96 h compared with glucose (control medium). Data were generated in PatternLab's AAPV module using a probability of 0.01. Green circle: glucose; yellow circle: *D. peruvianus* cuticle.

the sample and 10 mM riboflavin at the same time that tubes were placed under fluorescent light for 15 min. After this period, absorbance was determined at 560 nm. SOD unit was defined by NBT reduction per mL h<sup>-1</sup>.

Phosphatase activity was measured by the rate of *p*-nitrophenol (*p*-NP) production.<sup>11</sup> Samples were incubated for 60 min at room temperature in 0.2 mL of reaction mixture containing 116.0 mM NaCl, 5.4 mM KCl, 30.0 mM Hepes-Tris buffer pH 7.0, and 5.0 mM *p*-nitrophenylphosphate (*p*-NPP) as substrate. The reaction was stopped by the addition of 0.2 mL of 20% trichloroacetic acid. Subsequently, the reaction mixture was centrifuged at 1500g for 15 min at 25 °C. The absorbance was measured spectrophotometrically at 405 nm using a microplate reader SpectraMax (Molecular Devices, USA). The concentration of released *p*-nitrophenolate in the reaction was determined using a standard curve of *p*-nitrophenolate for comparison.

### Statistical Analysis

All enzymatic assays were performed in triplicate, with results obtained from at least three separate experiments. Data were analyzed statistically using the Student's *t* test and GraphPad Prism 5 software.

## RESULTS

### Bioassays

To confirm the ability of *M. anisopliae* to infect and kill *D. peruvianus*, we performed bioassays. One hundred percent mortality of *D. peruvianus* was observed 6 days after exposure to *M. anisopliae* conidia formulation (10<sup>8</sup> conidia mL<sup>-1</sup>) compared with 25% of the control (Figure S1 in the Supporting Information).

### Global Proteomic Analysis

Changes in the secreted proteome induced by exposure to host cuticle, (a model for infection condition) were identified by comparing to a control condition (glucose) at 48 and 96 h. Many more proteins were identified under the control condition, some overlapped, and others were unique to infection (Figure 1). Some important proteins related to cuticle degradation (proteases) and to defense and stress (catalase and SOD) were identified exclusively in the secretome mimicking infection condition (Table 1).

Of the proteins seen under both conditions, 14 and 10 proteins were identified as differentially regulated at 48 and 96 h of growth in *D. peruvianus* cuticle, respectively (Table 2). Among these, eight were considered up- and six down-regulated in 48 h, and

one up- and nine down-regulated for 96 h. The subtilisin protease Pr1B was the only protein up-regulated at both time points.

We also analyzed the media before exposure to fungus to detect background contamination from the media components. According to the results, we can eliminate the media as a source of contamination (Supplemental Table S1 in the Supporting Information).

Gene Ontology (GO) analyses provided a good view of *M. anisopliae* response to different conditions of growth. The GO annotations of differentially regulated and exclusive proteins are shown in Figure 2. Proteins containing hydrolase activity (34%) (including important virulence factors such as proteases), other functions (21%), and oxidoreductase activity (13%) were most abundant in 48 h. The same molecular functions were also identified in 96 h: hydrolase activity (22%), other (23%), and oxidoreductase activity (13%). Of the seven different proteins differentially regulated and annotated as hypothetical, we found four with conserved domains: tyrosinase (oxidoreductase activity); fungal lectine, related to immunomodulatory response, pyridoxamine 5'-phosphate oxidase, related to FMN binding; and endopeptidase (Table 3).

### Secretion Signals and Ortholog Analysis

A common concern in secretome analysis is the contamination by cellular lysis. As others have,<sup>14,39,40</sup> we addressed this issue by in silico scanning our identified proteins for secretion signals. We used multiple bioinformatic tools for a more complete data set.

Table S2 in the Supporting Information shows the predicted localization and possible secretion of all proteins identified as differentially expressed under infection condition. The analysis was done using six different programs: TargetP, SignalP, TMHMM, PredGPI, and WoLFPSORT following a pipeline, as already described,<sup>41</sup> and SECRETOOL as alternative analysis. According to the results, 45% of proteins were inferred as secreted, extracellular, or containing peptide signal sequence. During the infection process of fungal pathogens, the secretion of proteins that contain secretion signal could drop to only 56%.<sup>18</sup> The amount of 45% of proteins inferred as secreted or containing peptide signal in our work is in accordance with the average of the majority of the fungal secretomes, but even with some of the proteins lacking in silico evidence of secretion, such as SOD and ceramidase, they could be secreted by a nonclassical mechanism, such as through vesicles or by physiological wounding. It is possible also that some of these proteins could be products of mechanical wounding promoted by the mycelial agitation during

**Table 1. Exclusive Proteins Identified in *M. anisopliae* Supernatant When Grown in *D. peruvianus* Cuticle Medium for 48 and 96 h Compared with Culture Control (Glucose Medium)<sup>a</sup>**

accession no.	protein ID	spectral count	
		48 h	96 h
Biosynthetic Process			
gil322709716 gb EFZ01291.1	phosphatidylserine decarboxylase family protein	9	
gil322709871 gb EFZ01446.1	coproporphyrinogen III oxidase	6	39
gil322706303 gb EFY97884.1	putative agmatine deiminase		53
Catabolic Process			
gil322711930 gb EFZ03503.1	ABC transporter (Adp1)	10	17
Metabolic Process			
gil322708480 gb EFZ00058.1	amidohydrolase	106	71
gil322704296 gb EFY95893.1	subtilisin-like protease PrII	55	
gil322712004 gb EFZ03577.1	glutamate carboxypeptidase 2	47	
gil322705330 gb EFY96917.1	lactonohydrolase	25	27
gil322710784 gb EFZ02358.1	beta-galactosidase	15	26
gil322712543 gb EFZ04116.1	acetylornithine deacetylase	12	20
gil322703252 gb EFY94864.1	aspartic protease precursor	10	
gil322702995 gb EFY94612.1	YcaC amidohydrolase	7	
gil322707436 gb EFY99014.1	amidohydrolase	7	5
Oxidation–Reduction Process			
gil322707161 gb EFY98740.1	catalase	360	129
gil322705940 gb EFY97523.1	FAD binding domain protein	100	22
gil322705469 gb EFY97055.1	acyl-CoA dehydrogenase, putative	79	63
gil322705368 gb EFY96954.1	chitooligosaccharide oxidase	19	
gil322704839 gb EFY96430.1	fumarate reductase Osm1, putative		5
gil322712189 gb EFZ03762.1	superoxide dismutase		11
Proteolysis			
gil322705990 gb EFY97572.1	leupeptin-inactivating enzyme 1 precursor	172	56
Regulation			
gil322704735 gb EFY96327.1	G-protein beta subunit	50	30
gil322708390 gb EFY99967.1	regulatory P domain-containing protein	470	184
Unknown Function			
gil322705022 gb EFY96611.1	proteinase inhibitor I4	51	
gil322706303 gb EFY97884.1	putative agmatine deiminase	50	
gil322705292 gb EFY96879.1	carbohydrate-binding protein	22	
gil322702988 gb EFY94605.1	neutral ceramidase precursor	11	
Hypothetical Protein			
gil322706536 gb EFY98116.1	hypothetical protein MAA_06225	65	50
gil322705323 gb EFY96910.1	hypothetical protein MAA_07723	10	
gil322703203 gb EFY94816.1	hypothetical protein MAA_09749	9	7
gil322703687 gb EFY95292.1	hypothetical protein MAA_09241		10
gil322709650 gb EFZ01226.1	hypothetical protein MAA_03822	5	7

<sup>a</sup>Proteins were classified according to Gene Ontology.

culture or autolysis. However, as precisely pointed out in a *Botrytis cinerea* secretome study,<sup>42</sup> if cell lysis occurs, one would expect to observe many intracellular proteins that are known to have high abundance as internal mycelium proteins, and those specific proteins were not observed in our results. Moreover, as recently reviewed for fungal secretomes,<sup>18</sup> there are several lines of evidence indicating that various kinds of mechanistically distinct nonclassical export routes may exist and pathogenic fungi appear to have a particular feature lying in their ability to secrete proteins without canonical secretion signal. Also, different proteins known to be only cytoplasmic are being commonly identified in fungal secretomes, and their presence does not seem to result from artifacts (e.g., cell lysis); their functions in pathogenesis have not yet been identified.<sup>18</sup>

Table 4 shows the analysis of our secretome proteins and correspondent putative orthologs. Several proteins found in our work have matched with correspondent orthologs of other

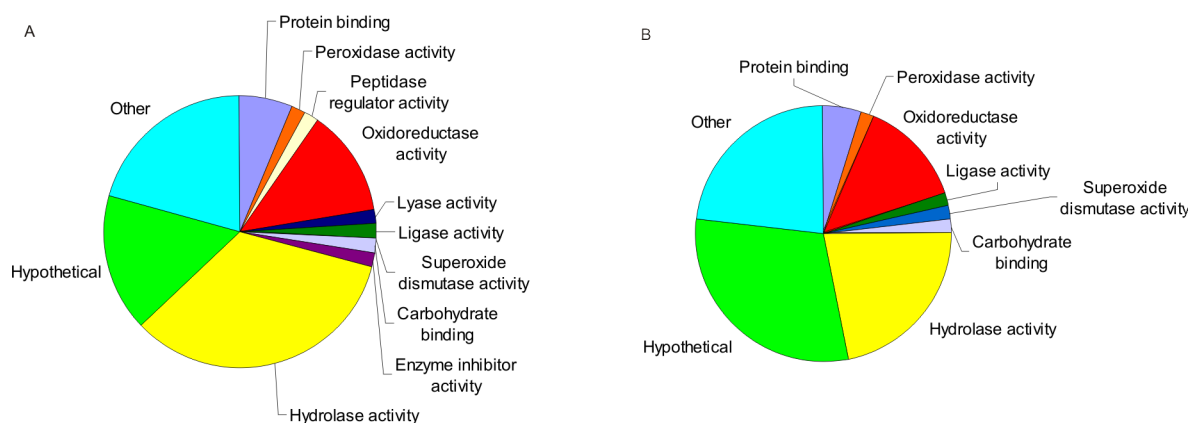
pathogenic fungi. Among the fungi that presented correspondent matches with *M. anisopliae* proteins, we could find different species being 50% matching to plant pathogens, around 10 and 37% to human pathogens and to other fungi considered non-pathogenic, respectively. Interestingly, one of the proteins, the proteinase inhibitor I4, has matched to a *Drosophila melanogaster* protein.

We also have made a comparison of our data to proteins identified in plant pathogens secretomes (Table 5). Because the infection processes of filamentous fungi entomopathogens and phytopathogens are very similar (in molecular compounds, host and fungal structures, penetration process, and enzyme secretion), it is very interesting to identify common and specific proteins secreted induced by specific host components. Several proteases, enzymes related to oxidative stress, phosphatases, and carbohydrate active enzymes were common to entomo- and phytopathogenic fungus.

**Table 2. Differentially Expressed Proteins Identified in *M. anisopliae* Supernatant Grown in *D. peruvianus* Cuticle Medium When Compared with Control (Glucose Medium Culture) for 48 and 96 h<sup>a,b</sup>**

accession number	fold change <sup>b</sup>	p value	protein ID	GO classification
48 h				
gil322704870 gb EFY96461.1	50.40	$9.11 \times 10^{-5}$	subtilisin-like protease Pr1B	metabolic process
gil322706957 gb EFY98536.1	25.65	$1.16 \times 10^{-5}$	subtilisin-like serine protease Pr1A	metabolic process
gil322711845 gb EFZ03418.1	18.38	0.000119	subtilisin-like serine protease Pr1C	metabolic process
gil322710850 gb EFZ02424.1	14.55	0.001615	1,2- $\alpha$ -D-mannosidase	metabolic process
gil322712350 gb EFZ03923.1	5.17	0.002486	leucine aminopeptidase, putative	metabolic process
gil322709036 gb EFZ00613.1	4.43	0.00297	glutamyl-tRNA(Gln) amidotransferase subunit A	metabolic process
gil322712549 gb EFZ04122.1	3.78	0.004866	cystein rich protein	
gil322705726 gb EFY97310.1	2.63	0.000208	protein tyrosine phosphatase	metabolic process
gil322708519 gb EFZ00097.1	-2.18	0.016227	5'-nucleotidase precursor	regulation
gil322706203 gb EFY97784.1	-2.77	0.000913	glucose-methanol-choline (gmc) oxidoreductase, putative	metabolic process
gil322703560 gb EFY95167.1	-3.63	0.001392	serine peptidase, putative	metabolic process
gil322711252 gb EFZ02826.1	-5.29	$2.91 \times 10^{-5}$	subtilisin-like serine protease Pr1J	metabolic process
gil322710325 gb EFZ01900.1	-10.95	0.000394	pyridine nucleotide-disulfide oxidoreductase family protein	proteolysis
gil322710287 gb EFZ01862.1	-12.06	$7.27 \times 10^{-5}$	eliciting plant response-like protein	
96 h				
gil322704870 gb EFY96461.1	2.34	0.007388	subtilisin-like protease Pr1B	metabolic process
gil322705726 gb EFY97310.1	-2.49	$7.88 \times 10^{-5}$	protein tyrosine phosphatase	metabolic process
gil322703407 gb EFY95016.1	-2.69	0.000111	hypothetical protein MAA_09465	
gil322709189 gb EFZ00765.1	-3.23	$1.00 \times 10^{-5}$	inorganic pyrophosphatase	oxidative process
gil322710982 gb EFZ02556.1	-3.52	$7.41 \times 10^{-5}$	endonuclease/exonuclease/phosphatase family protein	
gil322706059 gb EFY97641.1	-4.56	$1.89 \times 10^{-5}$	glycerophosphoryl diester phosphodiesterase family protein	metabolic process
gil322706203 gb EFY97784.1	-6.70	$1.00 \times 10^{-5}$	glucose-methanol-choline (gmc) oxidoreductase, putative	metabolic process
gil322703962 gb EFY95563.1	-7.85	0.001166	TRI14-like protein	
gil322709036 gb EFZ00613.1	-11.5	$1.00 \times 10^{-5}$	glutamyl-tRNA(Gln) amidotransferase subunit A	metabolic process
gil322710325 gb EFZ01900.1	-70.64	$1.00 \times 10^{-5}$	pyridine nucleotide-disulfide oxidoreductase family protein	proteolysis

<sup>a</sup>Proteins were differentially expressed statistically using PatternLab's TFold module, with an absolute fold change greater than 2.0. The proteins must be present in, at least, 4 replicates. <sup>b</sup>Based on spectral count numbers. Negative numbers represent down-regulated proteins in supernatant when grown on insect cuticle, compared to control condition.

**Figure 2.** Gene Ontology annotation. Molecular functions are represented at multilevel for differentially expressed proteins obtained from *M. anisopliae* supernatant when grown in *D. peruvianus* cuticle medium for (A) 48 or (B) 96 h.**Table 3. Putative Classification of *M. anisopliae* Hypothetical Proteins Identified under Infection Condition**

accession number	protein ID	culture time	differential expression level	conservative domain found <sup>a</sup>
gil322705323 gb EFY96910.1	hypothetical protein MAA_07723	48 h	exclusive	tyrosinase
gil322703203 gb EFY94816.1	hypothetical protein MAA_09749	48 and 96 h	exclusive	fungal lectine
gil322709650 gb EFZ01226.1	hypothetical protein MAA_03822	48 and 96 h	exclusive	pyridoxamine 5'-phosphate oxidase
gil322703687 gb EFY95292.1	hypothetical protein MAA_09241	96 h	exclusive	SCP-like extracellular protein/endopeptidase

<sup>a</sup>According to BLASTp search.

### Validation of Proteomic Data

Interestingly, some proteins identified in this paper were previously identified in other proteomic experiments related to

insect infection (Table S3 in the Supporting Information). Three proteases, Pr1A, I, and J, were identified in a previous study of *D. peruvianus*.<sup>12</sup> Enzymatic assays for protease and for other

Table 4. *M. anisopliae* Secreted Proteins and Its Correspondent Orthologs<sup>a</sup>

<i>M. anisopliae</i> protein name	OrthoMCL_group	organism	sequence name	e value	% identity	% match
Plant Pathogens						
subtilisin-like serine protease Pr1C	OG5_137388	<i>Fusarium graminearum</i>	conserved hypothetical protein	1e-181	58	99
eliciting plant response-like protein	OG5_152723	<i>Fusarium graminearum</i>	SnodProt1 precursor	2e-41	55	100
5'-nucleotidase precursor	OG5_127246	<i>Fusarium graminearum</i>	conserved hypothetical protein	1e-181	64	93
subtilisin-like serine protease Pr1A	OG5_128249	<i>Fusarium graminearum</i>	proteinase R precursor	1e-114	53	95
protein tyrosine phosphatase	OG5_126976	<i>Fusarium graminearum</i>	similar to protein tyrosine phosphatase	1e-181	79	99
acetylornithine deacetylase	OG5_127974	<i>Fusarium graminearum</i>	conserved hypothetical protein	1e-143	61	100
glutamate carboxypeptidase 2	OG5_128101	<i>Fusarium graminearum</i>	similar to prostate-specific membrane antigen	1e-181	67	100
ABC transporter (Adp1)	OG5_128747	<i>Fusarium graminearum</i>	protein similar to ABC transporter Adp1	1e-181	76	99
coproporphyrinogen III oxidase	OG5_128228	<i>Fusarium graminearum</i>	coproporphyrinogen III oxidase	1e-181	78	93
phosphatidylserine decarboxylase family protein	OG5_138667	<i>Fusarium graminearum</i>	similar to phosphatidylserine decarboxylase family protein	1e-102	43	97
hypothetical protein MAA_03822	OG5_142818	<i>Fusarium graminearum</i>	conserved hypothetical protein	2e-96	59	100
regulatory P domain-containing protein	OG5_149849	<i>Fusarium graminearum</i>	conserved hypothetical protein	1e-181	67	94
catalase	OG5_127182	<i>Fusarium graminearum</i>	catalase-3 precursor	1e-181	73	100
leupeptin-inactivating enzyme 1 precursor	OG5_209004	<i>Fusarium graminearum</i>	conserved hypothetical protein	1e-158	55	99
chitooglucosaccharide oxidase	OG5_139417	<i>Fusarium graminearum</i>	conserved hypothetical protein	1e-145	53	95
G-protein beta subunit	OG5_127516	<i>Fusarium graminearum</i>	similar to G-protein beta subunit	1e-179	95	100
subtilisin-like protease Pr1I	OG5_128249	<i>Fusarium graminearum</i>	proteinase R precursor	1e-110	53	95
YcaC amidohydrolase	OG5_133693	<i>Fusarium graminearum</i>	similar to protein ycaC	2e-91	64	98
endonuclease/exonuclease/phosphatase family protein	OG5_136984	<i>Fusarium graminearum</i>	similar to endonuclease/exonuclease/phosphatase family protein	1e-181	59	98
Inorganic pyrophosphatase	OG5_210486	<i>Fusarium graminearum</i>	conserved hypothetical protein	9e-75	49	96
glycerophosphoryl diester phosphodiesterase family protein	OG5_155948	<i>Fusarium graminearum</i>	glycerophosphoryl diester phosphodiesterase family	1e-151	59	99
hypothetical protein MAA_09465	OG5_152709	<i>Fusarium graminearum</i>	conserved hypothetical protein	4e-51	51	100
superoxide dismutase	OG5_127584	<i>Fusarium graminearum</i>	superoxide dismutase	3e-77	88	100
lactonohydrolase	OG5_133762	<i>Phytophthora ramorum</i>	ND	1e-139	65	99
Animal Pathogens						
cystein rich protein	OG5_188021	<i>Aspergillus fumigatus</i>	cysteine-rich secreted protein	1e-145	71	93
glutamyl-tRNA(Gln) amidotransferase subunit A	OG5_133516	<i>Aspergillus fumigatus</i>	amidase family protein, putative	1e-152	54	94
putative agmatine deiminase	OG5_134807	<i>Aspergillus fumigatus</i>	peptidyl-arginine deiminase superfamily	6e-67	39	98
acyl-CoA dehydrogenase, putative	OG5_169100	<i>Aspergillus fumigatus</i>	acyl-CoA dehydrogenase activity	1e-181	80	100
carbohydrate-binding protein	OG5_153045	<i>Coccidioides immitis</i>	carbohydrate-binding protein	3e-73	47	91
Other Fungi						
glucose-methanol-choline (gmc) oxidoreductase, putative	OG5_159842	<i>Aspergillus nidulans</i>	putative aryl-alcohol oxidase-related protein	1e-103	39	97
hypothetical protein MAA_07723	OG5_138597	<i>Aspergillus nidulans</i>	uncharacterized protein	1e-63	31	95
subtilisin-like serine protease Pr1J	OG5_129929	<i>Aspergillus oryzae</i>	subtilisin-related protease/Vacuolar protease B	2e-89	44	99
FAD binding domain protein	OG5_149814	<i>Aspergillus oryzae</i>	predicted protein	1e-181	66	99
hypothetical protein MAA_09749	OG5_209616	<i>Aspergillus oryzae</i>	predicted protein	1e-48	39	98
hypothetical protein MAA_06225	OG5_176924	<i>Laccaria bicolor</i>	ND	4e-09	39	87
hypothetical protein MAA_09241	OG5_127576	<i>Laccaria bicolor</i>	ND	2e-31	46	66
leucine aminopeptidase, putative	OG5_133339	<i>Neurospora crassa</i>	leucine aminopeptidase 2	1e-101	47	99
1,2-a-D-mannosidase	OG5_149768	<i>Neurospora crassa</i>	hypothetical protein	1e-143	51	93
pyridine nucleotide-disulfide oxidoreductase family protein	OG5_168989	<i>Neurospora crassa</i>	hypothetical protein	1e-181	57	88
subtilisin-like protease Pr1B	OG5_128249	<i>Neurospora crassa</i>	proteinase T	1e-101	52	94

Table 4. continued

<i>M. anisopliae</i> protein name	OrthoMCL_group	organism	sequence name	e value	% identity	% match
serine peptidase, putative	OG5_127 207	Plant Pathogens Other Fungi <i>Neurospora crassa</i> <i>Neurospora crassa</i> <i>Neurospora crassa</i> <i>Neurospora crassa</i> <i>Neurospora crassa</i> <i>Neurospora crassa</i> <i>Phanerochaete chrysosporium</i> Other <i>Drosophila melanogaster</i>	serine peptidase	1e-129	47	89
beta-galactosidase	OG5_132 459		beta-galactosidase	1e-181	53	99
amidohydrolase	OG5_133 329		amidohydrolase	2e-91	44	95
amidohydrolase	OG5_133 329		amidohydrolase	1e-133	55	99
neutral ceramidase precursor	OG5_129 670		neutral ceramidase	1e-118	57	100
fumarate reductase Osm1, putative	OG5_128 620		fumarate reductase Osm1	1e-181	86	100
aspartic protease precursor	OG5_144 197		ND	1e-24	29	91
proteinase inhibitor 14	OG5_126 693		ND	3e-34	33	90

<sup>a</sup>Analysis made using the OrthoMCL program.

enzymes were also applied to further validate the proteomic data. Table 6 shows that the enzymatic activity results are in accordance with the proteomic results. For proteases we used two  $\rho$ NA substrates: general protease and the specific Pr1 activity were higher when *M. anisopliae* was grown in culture media, mimicking the infection condition for both times analyzed.

Phosphatase activity in 48 h and catalase and SOD activities were also higher under infection conditions than under control conditions.

The identification and validation of known secretome components supports the use of the experimental design presented in this work to identify infection-related secreted proteins.

### Protein Interaction Networks

To evaluate the network of those differentially regulated proteins identified exclusively under infection conditions (cuticle secretome), we generated interaction networks. For the 48h time point, 24 proteins (58%) were identified (Figure 3A). We observed that one protein represents the majority of connections: the serine protease Pr1C. This protein was identified as up-regulated under infection conditions and was able to form 11 connections with several other proteases, including Pr1A, B, I, and J (Figure 3B). It is therefore tempting to speculate that the physiological interaction between these proteins might contribute to the cooperation or coordination of their functions in the degradation of proteinaceous arthropod cuticle layer. Evaluating the network by the highest score, that is, closest similarity in the ontological distance, we identified three groups. The first group related to protein degradation (Pr1A, I, and J), the second group with two proteins related to oxidation and FAD binding, and the third group related to sugar degradation (Figure 3C).

When the 96h network was analyzed, 40% of the proteins had predicted interactions (Figure 4). When compared with the 48 h time point, it was not possible to identify any clusters of proteins with multiple connections. All 12 proteins interact with one or two other proteins. However, the highest score was observed for the same group that already appears in the 48 h time point, functions related to sugar degradation, suggesting the importance of these proteins in glucose uptake for fungal growth.

## DISCUSSION

Evaluating the secretion of proteins during the growth of microbial pathogens under artificial infection conditions could reveal strategies and the components responsible for the success of the host infection and colonization. The strategy of applying synthetic media to induce the activation of the infection systems has been applied with success, revealing genes and proteins involved in different stages of *Metarhizium anisopliae*'s infection process.<sup>7,12,43,44</sup> Several articles have been reporting poor correlation between mRNA and protein levels.<sup>45–47</sup> Most of the work in *M. anisopliae* has analyzed gene expression, which makes the identification of secreted proteins difficult.<sup>48</sup> Proteomics data is closer to the biologically active processes and should therefore be used to investigate biological phenomena and mechanisms, and it can be used to measure the presence of proteins in subcellular locations.<sup>49</sup> Only a few proteomic studies have been published on *M. anisopliae* and all applied low-throughput techniques.<sup>12,43,50–54</sup> By applying shotgun proteomics,<sup>21</sup> we were able to identify 71 proteins differentially expressed under infection conditions. Most of these proteins were not detected in other proteomic experiments about insect infection.<sup>12,43,52,53</sup> Multiple molecular functions were assigned to these 71 proteins by GO annotation, including several known to be involved in *M. anisopliae* infection



Table 5. Shared Proteins between Fungal Plant Pathogens and *M. anisopliae* Secretomes

fungus	references	shared proteins	exclusive proteins MA - this work
<i>Botrytis cinerea</i>	Fernández-Acero et al. 2010 <sup>a</sup> Li et al. 2012 <sup>b</sup> Espino et al. 2010 <sup>c</sup> Shah et al. 2009 <sup>d</sup> Shah et al. 2009 <sup>e</sup> Shah et al. 2012 <sup>f</sup>	phosphatase aspartic protease carboxypeptidase FAD binding protease serine protease aminopeptidase oxidoreductase mannosidase galactosidase	S'-nucleotidase precursor acetylornithine deacetylase acyl-CoA dehydrogenase, putative carbohydrate-binding protein chitooligosaccharide oxidase coproporphyrinogen III oxidase cystein rich protein eliciting plant response-like protein fumarate reductase Osm1, putative glutamyl-tRNA(Gln) amidotransferase subunit A glycerophosphoryl diester phosphodiesterase family protein G-protein beta subunit pyridoxamine 5'-phosphate oxidase <sup>g</sup> hypothetical protein MAA_06225 SCP-like extracellular protein/endopeptidase <sup>i</sup> hypothetical protein MAA_09465 fungal lectine <sup>j</sup> lactonohydrolase leupeptin-inactivating enzyme 1 precursor neutral ceramidase precursor phosphatidylserine decarboxylase family protein protease inhibitor I4 putative agmatine deiminase regulatory P domain-containing protein subtilisin-like protease Pr1B subtilisin-like protease PR11 subtilisin-like serine protease PR1A subtilisin-like serine protease PR1C subtilisin-like serine protease PR1J TRI14-like protein
<i>Fusarium graminearum</i>	Yang et al. 2012 <sup>g</sup> Rampitsch et al. 2013 <sup>h</sup>	protease aminopeptidase carboxypeptidase GMC-oxidoreductase catalase endonuclease/exonuclease/phosphatase family serine protease SOD amidohydrolase	
<i>Magnaporthe oryzae</i>	Jung et al. 2012 <sup>j</sup> Kim et al. 2013 <sup>k</sup>	ABC-transporter FAD binding tyrosinase carboxypeptidase subtilisin-like protease SOD aminopeptidase	
<i>Mycosphaerella graminicola</i>	Morais do Amaral et al. 2012 <sup>l</sup>	aspartic protease serine protease carboxypeptidase peptidase mannosidase GMC-oxidoreductase tyrosinase FAD binding	

<sup>a</sup>Fernández-Acero et al. *Proteomics* **2010**, 10 (12), 2270–80. <sup>b</sup>Li et al. *J. Proteome Res.* **2012**, 11 (8), 4249–4260. <sup>c</sup>Espino et al. *Proteomics* **2010**, 10 (16), 3020–3034. <sup>d</sup>Shah et al. *Proteomics* **2009**, 9 (11), 3126–3135. <sup>e</sup>Shah et al. *J. Proteome Res.* **2012**, 11 (4), 2178–2192. <sup>f</sup>Shah et al. *J. Proteome Res.* **2009**, 8 (3), 1123–1130. <sup>g</sup>Yang et al. *Mol Plant Pathol.* **2012**, 13 (5), 445–453. <sup>h</sup>Rampitsch et al. *Proteomics* **2013**, 13 (12–13), 1913–1921. <sup>i</sup>Hypothetical protein reclassified according to Table 3. <sup>j</sup>Jung et al. *Proteomics* **2012**, 12 (6), 878–900. <sup>k</sup>Kim et al. *J. Proteomics* **2013**, 78, 58–71. <sup>l</sup>Morais do Amaral et al. *PLoS One* **2012**, 7 (12), e49904.

Table 6. Validation of Proteomic Results Using Enzymatic Assays

enzymatic assay	time (h)	culture media	
		DP <sup>a</sup>	G <sup>b</sup>
phosphatase	48	79.1 ± 3.1 <sup>c</sup>	5.3 ± 0.6
catalase	48	0.87 ± 0.08 <sup>d</sup>	0.47 ± 0.02
	96	0.85 ± 0.08 <sup>c</sup>	0.4 ± 0.08
SOD	96	1818 ± 217 <sup>c</sup>	457 ± 44
BAPNA (Bz-DL-Arg-pNA)	48	0.01 ± 0.003 <sup>c</sup>	0.002 ± 0.0003
	96	0.007 ± 0.0004 <sup>c</sup>	0.002 ± 0.0004
Pr1 (N-suc-ala-ala-pro-phe-pNA)	48	2.59 ± 0.27 <sup>c</sup>	0.14 ± 0.03
	96	2.76 ± 0.16 <sup>c</sup>	0.094 ± 0.03

<sup>a</sup>DP: *Dysdercus peruvianus* cuticle. <sup>b</sup>G: glucose. <sup>c</sup> $p < 0.001$ . <sup>d</sup> $p < 0.005$ .

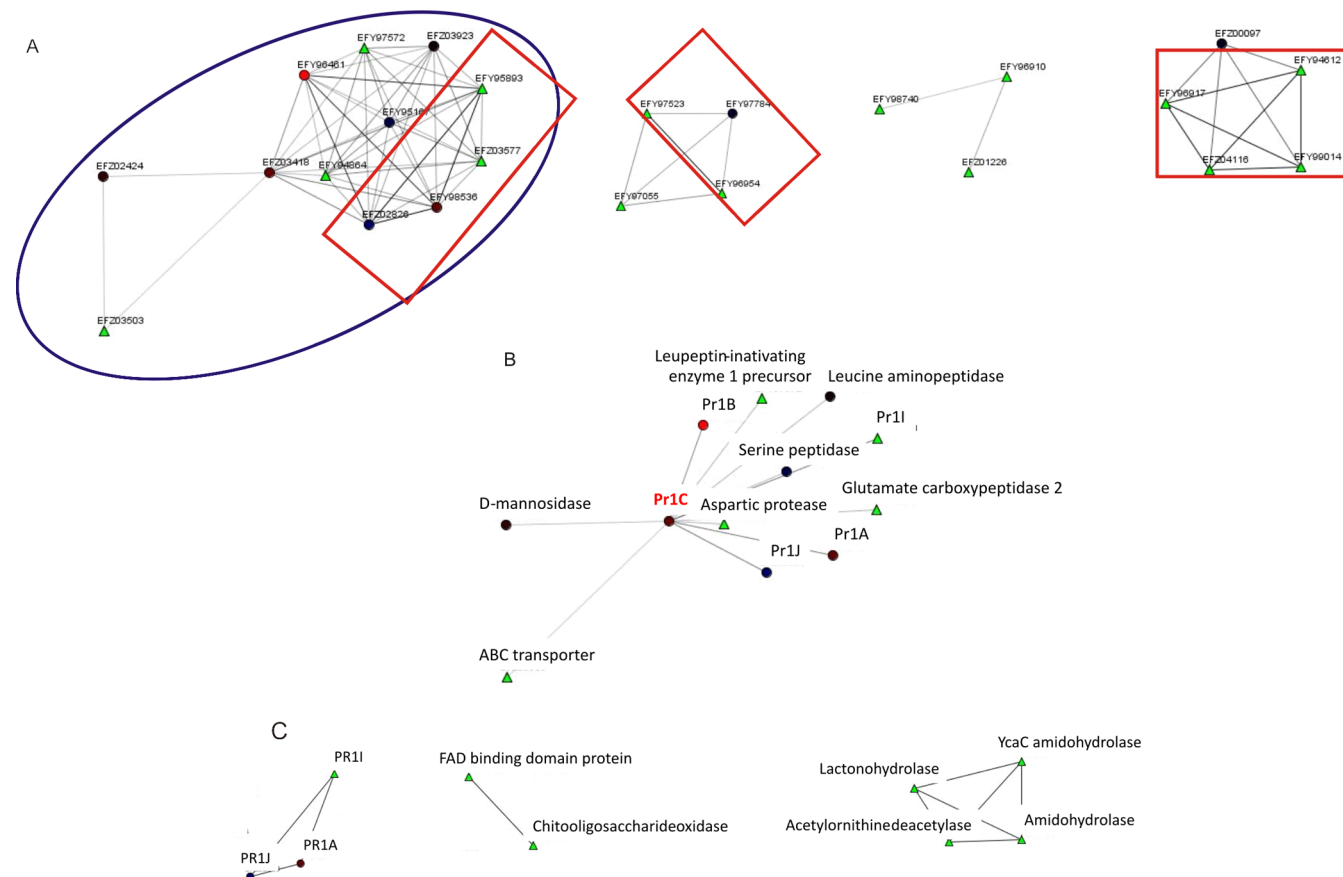


**Figure 3.** Network analysis of differentially expressed proteins identified in 48h *M. anisopliae* supernatant when grown *D. peruvianus* cuticle medium. (A) Total integrative network. (B) Cluster identifying proteins with higher connectivity: blue circle shown in panel A. (C) Clusters showing higher score or strong interaction: red rectangles shown in panel A. Spheres and triangles represent proteins; lines connecting spheres indicate interactions between proteins. Red spheres, proteins up-regulated in response to DP cuticle; blue spheres, proteins down-regulated; green triangles, exclusive proteins identified in DP cuticle.

(hydrolase activity, enzyme inhibitor activity, oxidoreductase activity, superoxide dismutase activity, and protein and carbohydrate binding).<sup>6–9</sup>

The infection process occurs in three stages: (1) adhesion to the cuticle, (2) penetration of the cuticle, followed by (3) host colonization of the internal tissues. In this study, we addressed the secreted proteins induced by interactions with the host cuticle that are involved mainly in the second stage. For these stages, cuticle-degrading enzymes, virulence factors, and proteins related to nutrient acquisition were identified. In addition to many previously reported proteins that play key roles in host infection, here we report several additional new potential factors

that could also play key roles in the important biological process of infection; suggesting that the proteins may be attempting to manage the host response to infection. Interestingly, we see this fungal action in the absence of an active host defense system.

### Cuticle-Degrading Enzymes

Secretion of enzymes causing cuticle disruption enables penetration and gives a strong advantage to pathogens.<sup>12,55</sup> Lipolytic enzymes have been described as essential for *M. anisopliae* infection, mainly in early stages.<sup>6–8</sup> Consistent with this finding, we identified lactonohydrolase and neutral ceramidase only at 48 h. These enzymes are very specific, which is important considering the high complexity of lipids present in different host

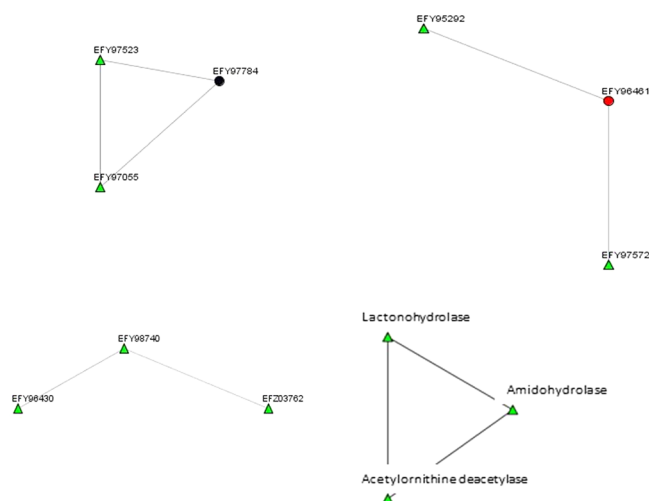


**Figure 4.** Network analysis of differentially expressed proteins identified in 96h *M. anisopliae* supernatant when grown *D. peruvianus* cuticle medium. Spheres and triangles represent proteins; lines connecting spheres indicate interactions between proteins. Red spheres, proteins up-regulated in response to DP cuticle; blue spheres, proteins down-regulated; green triangles, exclusive proteins identified in DP cuticle.

cuticles.<sup>1</sup> This activity may be required for multiple stages of infection.<sup>8</sup> Moreover, ceramidase activity was reported to enhance phospholipase C activity in microbial pathogens.<sup>56</sup> Phospholipase C is a classic microbial virulence factor that has been detected in *M. anisopliae*.<sup>8</sup>

Among the degradative enzymes of *M. anisopliae*, proteases are crucial for the infection because they are required to break through the protein containing cuticle and prepare the host proteins in the hemolymph for absorption as nutrients.<sup>1</sup> Five members of the subtilisin-like serine proteases family, Pr1, were differentially expressed. This enzyme class is the most extensively studied and best understood in entomopathogenicity and may also influence virulence or host specificity.<sup>1,12,43,57</sup> Pr1A was previously detected in other proteomics studies about *M. anisopliae* infection in different hosts, including *Callosobruchus maculatus*, *Rhizoglyphus microplus*, and also *Dysdercus peruvianus*.<sup>12,43,50</sup> Therefore, this protease is related to host infection but not to host specificity. We expected that Pr1A would be the predominant protein produced during degradation of insect cuticles because ESTs for *Pr1A* are 10 times more abundant than the second most highly expressed sequence (*Pr1J*).<sup>58</sup> We found that Pr1A was highly increased; however, the increase in another serine protease, Pr1B, was even greater. Surprisingly, Pr1J was not similarly up-regulated. It is crucial to remember that the levels of transcripts and translated proteins are sometimes imperfectly associated,<sup>47,59</sup> and assumptions based at RNA expression level can be very wrong because the real players in the infection systems are the proteins. Proteases, such as Pr1A and B, were also described as part of a general response to nutrient deprivation.<sup>44</sup> Other Pr1 proteases previously identified in *D. peruvianus* infection were also identified in this work: Pr1I and J.<sup>12</sup> According to our results Pr1J was the only serine protease down-regulated in 48 h, being secreted together with other 4 Pr1 proteases (Pr1A, B, C, and I), which were up-regulated at the same time. This differential expression among different Pr1 proteases could be related to host specificity and different cuticle composition during the infection.<sup>12</sup> As previously discussed, degradation products function as specialized signals, allowing the fungus to “sample” the cuticle and then respond with the

secretion of specific proteins.<sup>44</sup> This feedback also could explain the huge difference in the fold change of Pr1B between 48 and 96 h. The dynamic interaction requires that different proteases in different amounts are employed at different moments during infection. Other proteases, protease inhibitor I4 and leupeptin inactivating enzyme, were also identified and could be closely related to this complex proteolytic system. The proteomic data are in accordance with the enzymatic assays. The assays with the specific substrate for Pr1 presented remarkably higher activity under infection condition compared with the control condition. On the basis of our results and data previously published,<sup>12,44</sup> it is obvious that each protease could have different biological and functional roles. We believe the fungus is continuously sampling the environment and adjusts its secretions accordingly.

We were interested in determining if the identified proteins act in complexes or networks. We could not perform coimmunoprecipitation experiments due to the lack of available antibodies. Therefore, we developed an *in silico* approach to identify proteins with similar profiles. Beyond the independent role of each protease/protein during the infection, our integrative interaction results provide new insight and a wider view into the *M. anisopliae* infection system. Pr1C occupies a central position in the largest cluster of proteins at 48 h. Because this protein presents the highest number of interaction nodes, its up-regulation could be secondary in relevance for the system compared with a possible regulatory and interactive role with several other important proteins. Also, the proteins Pr1A, I, and J show different expression levels, but they present the strongest interaction forces forming an internal cluster in the large proteolytic cluster at 48 h. In this way, the results can rank possible targets for future studies and also identify important proteins independently of their expression levels. In all previous studies, the main conclusions were always made from proteins/genes up-regulated, and obviously some regulatory players could be missed due to the limitations of this limited analysis over the complexity of the system.

### Fungal Protection/Manipulation of Redox State and Signaling

Another set of interesting proteins are enzymes involved in protection against reactive oxygen species (ROS). Catalases and superoxide dismutases (SOD), classical examples of these proteins, were identified in our proteomic results and validated in enzymatic assays and reported in previous studies. (See Table S3 in the Supporting Information.) Catalases and SODs associated with *M. anisopliae* conidia have been shown to be involved in protection against UV radiation.<sup>8</sup> Because attempted penetration by filamentous pathogens is known to provoke ROS production by the host,<sup>60</sup> we did not expect to see these proteins in our artificial infection condition because the insect is dead and cannot elicit a defensive response. So the question remains, why are these being secreted? There is growing evidence that ROS are important for many aspects of fungal life, including infection, structure formation, cellular communication and signaling, and ecological process.<sup>61</sup> Among all differentially expressed proteins identified, several of them are classified in oxidoreductase activity molecular function according to GO annotation. Oxidoreductases are related to alteration of redox state of the host, which can perturb host gene expression in response to environmental stress such as fungal growth.<sup>62</sup> It is possible that oxidoreductase activity combined with up-regulation of SOD and catalase alters the regulation of the redox system of the host during the infection. This possible interaction was detected in our network results, where SOD and fumarate reductase were both interacting with

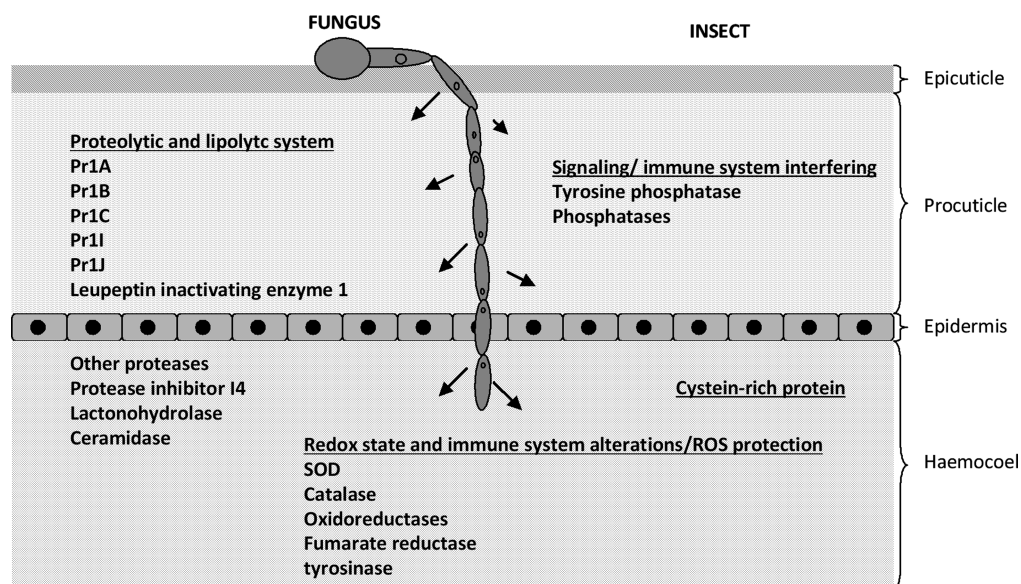


**Figure 5.** Proposed schematic model of fungal effectors and other proteins expressed by *M. anisopliae* during *D. peruvianus* infection, according to proteomic data.

catalase. Tyrosinase, another protein traditionally associated with UV resistance of conidia, was also up-regulated in infection. In *Beauveria bassiana*, this protein is thought to have a role in virulence in later stages of infection.<sup>63</sup> There is a growing body of evidence that in addition to the well-established roles for these proteins in stress tolerance and protection in the host these proteins appear to have a new role in fungal virulence.<sup>64,65</sup> Unfortunately, the molecular role of these proteins in this process is still unclear. For instance, ROS play a major role in phytopathogens infection, a very similar system to entomopathogens, and even in this system the specific role of these molecules is not well understood.<sup>66</sup> One possibility is that the differential expression of these proteins could manipulate the host redox system to alter host signaling mechanisms and defense response.

### Signaling

Other signaling-related proteins with roles in microbial infection were identified. G proteins are a family of proteins involved in transmitting signals from outside the cell to inside the cell.<sup>67</sup> In *M. anisopliae*, this protein was previously characterized, playing roles in regulation of conidiation, virulence, and adhesion, modulating its ability to respond to environmental stimuli.<sup>68</sup> Interestingly, in this work, only the beta subunit was detected and probably is related to an unknown function outside the fungal cell. Tyrosine phosphatase, up-regulated at 48 h and down-regulated at 96 h, together with other phosphatases, also plays critical roles in signaling and biotic stress. These enzymes were previously described as secreted microbial virulence factors targeting host-cell immune responses.<sup>69</sup> Specifically, *M. anisopliae* tyrosine phosphatase interferes with insect innate immune response to microbial infection, dephosphorylating phosphoproteins involved in protein transport in insect hemolymph.<sup>70</sup> Moreover, phosphatase activity was also shown to be one of the mediators of the adhesion process on the host surface,<sup>11</sup> and possibly these enzymes are playing multiple roles during different times of the infection out and inside the host.

### Fungal Effectors and Comparison to Plant Pathogens

Extracellular effectors are defined as small molecules and proteins secreted by pathogens into the host where they alter host-cell structure and function.<sup>71</sup> Some of these proteins are well known

and are previously characterized fungal effectors and or signaling interfering proteins that can act on host metabolites or proteins, possibly modifying responses to fungal infection in benefit to the pathogen.<sup>64,65,67,72</sup> Unrelated fungal pathogens secrete the same effectors for creating a more compatible host environment, including mechanisms to manipulate host-cell metabolism.<sup>72</sup> The effector repertoire includes several proteins previously identified and described: glycosyl hydrolases, proteases, ROS-related proteins, among others (Figure 5). Another classical effector,<sup>71,73</sup> the cysteine-rich protein, was also identified. The combination of all proteins identified during the artificial activation of the infection system could reveal that *M. anisopliae* is not only degrading and consuming host components but also is actively modulating host physiology by the secretion of different proteins. Also, as presented in Table 4, the proteins found in our study presented orthologs in several different fungal pathogens, which is possible evidence of correlation and conservation of different pathogenic systems linked to different hosts. According to this analysis of putative orthologs, the proteinase inhibitor I4 had the best match corresponding to a *Drosophila melanogaster* protein, which reinforces the idea that the fungus is possibly actively interfering the host response. This inhibitor having the best match corresponding to an arthropod protein could probably be because it inhibits proteases expressed by the host, an arthropod, during the infection.

Because the infection processes of filamentous fungi entomopathogens and phytopathogens are very similar (in molecular compounds, host and fungal structures, penetration process, and enzyme secretion), it is very interesting to identify common and specific proteins secreted induced by specific host components. Among the shared proteins are several proteases, enzymes related to oxidative stress, phosphatases, and carbohydrate active enzymes. Also, according to the analysis made to check ortholog proteins, half of the proteins identified have the best match for correspondent orthologs in phytopathogens, which are 47.9% proteins from *Fusarium graminearum*. With this result, the idea that these two similar pathogenic systems are evolutionarily conserved is in accordance. The FAD binding domain protein is also shared, and although it contains a predicted secretion signal, its extracellular role is unexpected and currently unknown.



However, FAD binding domains are considered to be one of the most frequent PFAM domains found throughout the secretome of two important filamentous fungi plant pathogens, *Fusarium graminearum* and *Mycosphaerella graminicola*, and are also detected in *B. cinerea* secretome, other important plant pathogen, reinforcing our result and the similarity of both pathogenic systems.<sup>14,74</sup> Some of the 30 proteins exclusively identified in *M. anisopliae* were already described in plant pathogens with a role in infection, as cysteine-rich protein, for instance, but not yet detected in secretome studies. Because secretome data for fungal entomopathogens are still limited, this difference to plant pathogens could be a very interesting approach to understand the specificity of both systems.

It is important to highlight also that according to the result presented we found orthologs matching to human pathogens, most of the proteins matching to *Aspergillus fumigatus*, and around 37% matching to other fungi considered nonpathogenic, like *Aspergillus nidulans* and *Neurospora crassa*. Specifically, the proteins with the best match for nonpathogenic fungi proteins are also interesting targets for future studies due to this close similarity to nonpathogens. These proteins could be specific for the infection of *M. anisopliae*'s host and expressed along with proteins also expressed by other pathogenic fungi, allowing the success of the infection.

## CONCLUSIONS

In this work, we presented a new view into *M. anisopliae*'s infection system using, for the first time, shotgun proteomics and interaction network analysis. The differential expression of several proteins other than just a few degrading enzymes and other already expected and previously known proteins was accessed. Using the insect model *D. peruvianus* and the induction of the infection system by a host cuticle, it is now possible to learn that fungus secretes different proteins that can act over different substrates within host environment, possibly altering host response and preparing an improved condition for fungal colonization. Among these several proteins, hypothetical and unknown proteins were found. For instance, the protein quantified with the highest spectral count in 48 and 96 h, the regulatory P domain protein, according to genome annotation, is actually a hypothetical protein according to BLASTP and probably has an important role in *D. peruvianus* infection; by using network analysis techniques, we could integrate part of secreted proteome. This strategy could provide a way to target proteins for future studies, analyzing not only expression changes during infection but also its interaction with other secreted proteins. Microbial infection is a complex process between the host and the pathogen, and further investigation of each protein identified and its specific role in this complex system is necessary. Although each host can trigger different molecular responses, *M. anisopliae*'s infection strategy against the insect *D. peruvianus* looks very similar to other unrelated pathogenic fungi because all fungi need to prepare the host for a successful infection. Other proteins presenting orthologs in nonpathogenic fungi are also interesting targets for future studies because it could be the difference of the entomopathogenic system compared with other infection systems. The results presented here are a relevant advance in the understanding of this particular host–pathogen interaction process and may be applicable to the search for more efficient strains and to develop new formulations to control the cotton pest *D. peruvianus*.

## ASSOCIATED CONTENT

### Supporting Information

S1. Glucose as control condition. S2. Networks. Table S1. Proteins identified in culture medium without fungal growth. Table S2. Localization prediction of proteins identified as differentially expressed in *M. anisopliae* supernatant when grown in *D. peruvianus* cuticle medium for 48 and 96 h. Table S3. Proteins identified previously reported by other proteomic works in *M. anisopliae* host–pathogen interaction related to insects. Figure S1. Effect of *M. anisopliae* on *D. peruvianus* adults over time. This material is available free of charge via the Internet at <http://pubs.acs.org>.

## AUTHOR INFORMATION

### Corresponding Author

\*Phone: +1 (858) 784-3076. Fax: +1 (858) 784-8883. E-mail: [wbeys@scripps.edu](mailto:wbeys@scripps.edu); [walterbeys@yahoo.com.br](mailto:walterbeys@yahoo.com.br).

### Notes

The authors declare no competing financial interest.

## ACKNOWLEDGMENTS

We thank Dr. Augusto Schrank who kindly provided the *M. anisopliae* strain, Dr. Celia Carlini who kindly provided the insects used in this work, and Dr. Jeffrey Savas for technical advice. J.J.M. and J.R.Y. were supported by the National Center for Research Resources (SP41RR011823-17), National Institute of General Medical Sciences (8 P41 GM103533-17), National Heart, Lung, and Blood Institute (HHSN268201000035C), and National Institute on Aging (R01AG027463-04). This work was also supported by grants from the following Brazilian agencies: Conselho Nacional de Desenvolvimento Científico e Tecnológico (CNPq) and Coordenação de Aperfeiçoamento de Pessoal de Nível Superior (CAPES). W.O.B.-d.-S. and L.S. are fellows from Brazilian program Ciência Sem Fronteiras, CAPES.

## REFERENCES

- (1) Beys-da-Silva, W. O.; Santi, L.; Vainstein, M. H.; Schrank, A. Biocontrol of the Cattle Tick *Rhipicephalus (Boophilus) microplus* by the Acaricidal Fungus *Metarhizium anisopliae*. In *Ticks: Disease, Management and Control*; Woldemeskel, M., Ed.; Nova Science Publishers, Inc.: Hauppauge, NY, 2012; pp 217–246.
- (2) Beys-da-Silva, W. O.; Santi, L.; Berger, M.; Guimarães, J. A.; Schrank, A.; Vainstein, M. H. Susceptibility of *Loxosceles* sp. to the arthropod pathogenic fungus *Metarhizium anisopliae*: potential biocontrol of the brown spider. *Trans. R. Soc. Trop. Med. Hyg.* **2013**, *107* (1), 59–61.
- (3) Hernandez, C. E. M.; Guerrero, I. E. P.; Hernandez, G. A. G.; Solis, E. S.; Guzman, J. C. T. Catalase overexpression reduces the germination time and increases the pathogenicity of the fungus *Metarhizium anisopliae*. *Appl. Microbiol. Biotechnol.* **2010**, *87*, 1033–1044.
- (4) Santi, L.; Silva, L. A. D.; Silva, W. O. B.; Correa, A. P. F.; Rangel, D. E. N.; Carlini, C. R.; Schrank, A.; Vainstein, M. H. Virulence of the entomopathogenic fungus *Metarhizium anisopliae* using soybean oil formulation for control of the cotton stainer bug, *Dysdercus peruvianus*. *World J. Microbiol. Biotechnol.* **2011**, *27*, 2297–2303.
- (5) Midega, C. A.; Nyang'au, I. M.; Pittchar, J.; Birkett, M. A.; Pickett, J. A.; Borges, M.; Khan, Z. R. Farmers' perceptions of cotton pests and their management in western Kenya. *Crop Prot.* **2012**, *42*, 193–201.
- (6) Beys da Silva, W. O.; Santi, L.; Schrank, A.; Vainstein, M. H. *Metarhizium anisopliae* lipolytic activity plays a pivotal role in *Rhipicephalus (Boophilus) microplus* infection. *Fungal Biol.* **2010**, *114* (1), 10–15.
- (7) Beys da Silva, W. O.; Santi, L.; Corrêa, A. P.; Silva, L. A.; Bresciani, F. R.; Schrank, A.; Vainstein, M. H. The entomopathogen *Metarhizium*

*anisopliae* can modulate the secretion of lipolytic enzymes in response to different substrates including components of arthropod cuticle. *Fungal Biol.* **2010**, *114* (11–12), 911–916.

(8) Santi, L.; Beys da Silva, W. O.; Berger, M.; Guimarães, J. A.; Schrank, A.; Vainstein, M. H. Conidial surface proteins of *Metarhizium anisopliae*: Source of activities related with toxic effects, host penetration and pathogenesis. *Toxicon* **2010**, *55*, 874–880.

(9) Silva, W. O. B.; Santi, L.; Berger, M.; Pinto, A. F. M.; Guimaraes, J. A.; Schrank, A.; Vainstein, M. H. Characterization of a spore surface lipase from the biocontrol agent *Metarhizium anisopliae*. *Proc. Biochem.* **2009**, *44*, 829–834.

(10) Broetto, L.; Da Silva, W. O. B.; Bailão, A. M.; De Almeida Soares, C.; Vainstein, M. H.; Schrank, A. Glyceraldehyde-3-phosphate dehydrogenase of the entomopathogenic fungus *Metarhizium anisopliae*: cell-surface localization and role in host adhesion. *FEMS Microbiol. Lett.* **2010**, *312* (2), 101–109.

(11) Cosentino-Gomes, D.; Rocco-Machado, N.; Santi, L.; Broetto, L.; Vainstein, M. H.; Meyer-Fernandes, J. R.; Schrank, A.; Beys-da-Silva, W. O. Inhibition of ecto-phosphatase activity in conidia reduces adhesion and virulence of *Metarhizium anisopliae* on the host insect *Dysdercus peruvianus*. *Curr. Microbiol.* **2013**, *66*, 467–474.

(12) Santi, L.; Silva, W. O. B.; Pinto, A. F.; Schrank, A.; Vainstein, M. H. *Metarhizium anisopliae* host-pathogen interaction: differential immunoproteomics reveals proteins involved in the interaction process of arthropods. *Fungal Biol.* **2010**, *114*, 312–319.

(13) Silva, W. O. B.; Mitidieri, S.; Schrank, A.; Vainstein, M. H. Production and extraction of an extracellular lipase from the entomopathogenic fungus *Metarhizium anisopliae*. *Proc. Biochem.* **2005**, *40*, 321–326.

(14) Fernández-Acero, F. J.; Colby, T.; Harzen, A.; Carbú, M.; Wieneke, U.; Cantoral, J. M.; Schmidt, J. 2-DE proteomic approach to the *Botrytis cinerea* secretome induced with different carbon sources and plant-based elicitors. *Proteomics* **2010**, *10* (12), 2270–2280.

(15) Suárez, M. B.; Sanz, L.; Chamorro, M. I.; Rey, M.; González, F. J.; Llobell, A.; Monte, E. Proteomic analysis of secreted proteins from *Trichoderma harzianum*. Identification of a fungal cell wall-induced aspartic protease. *Fungal Genet. Biol.* **2005**, *42* (11), 924–934.

(16) Phalid, V.; Delalande, F.; Carapito, C.; Goubet, F.; Hatsch, D.; Leize-Wagner, E.; Dupree, P.; Dorselaer, A. V.; Jeltsch, J. M. Diversity of the exoproteome of *Fusarium graminearum* grown on plant cell wall. *Curr. Genet.* **2005**, *48* (6), 366–379.

(17) Espino, J. J.; Gutiérrez-Sánchez, G.; Brito, N.; Shah, P.; Orlando, R.; González, C. The *Botrytis cinerea* early secretome. *Proteomics* **2010**, *10* (16), 3020–3034.

(18) Girard, V.; Dieryckx, C.; Job, C.; Job, D. Secretomes: the fungal strike force. *Proteomics* **2013**, *13* (3–4), 597–608.

(19) Yang, F.; Jensen, J. D.; Svensson, B.; Jorgensen, H. J.; Collinge, D. B.; Finnie, C. Secretomics identifies *Fusarium graminearum* proteins involved in the interaction with barley and wheat. *Mol. Plant Pathol.* **2012**, *13* (5), 445–453.

(20) Smith, P. K.; Krohn, R. I.; Hermanson, G. T.; Mallia, A. K.; Gartner, F. H.; Provenzano, M. D. Measurement of the principle of protein-dye binding. *Anal. Biochem.* **1985**, *150*, 76–85.

(21) Washburn, M. P.; Wolters, D.; Yates, J. R., 3rd. Large-scale analysis of the yeast proteome by multidimensional protein identification technology. *Nat. Biotechnol.* **2001**, *19* (3), 242–247.

(22) McDonald, W. H.; Tabb, D. L.; Sadygov, R. G.; MacCoss, M. J.; Venable, J.; Graumann, J.; Johnson, J. R.; Cociorva, D.; Yates, J. R. MS1, MS2, and SQT-three unified, compact, and easily parsed file formats for the storage of shotgun proteomic spectra and identifications. *Rapid Commun. Mass Spectrom.* **2004**, *18* (18), 2162–2168.

(23) Xu, T.; Venable, J. D.; Park, S. K.; Cociorva, D.; Lu, B.; Liao, L.; Wohlschlegel, J.; Hewel, J.; Yates, J. R. ProLuCID, a fast and sensitive tandem mass spectra-based protein identification program. *Mol. Cell. Proteomics* **2006**, *5*, S174.

(24) Tabb, D. L.; McDonald, W. H.; Yates, J. R., 3rd. DTASelect and Contrast: tools for assembling and comparing protein identifications from shotgun proteomics. *J. Proteome Res.* **2002**, *1*, 21–26.

(25) Eng, J. K.; McCormack, A. L.; Yates, J. R., III. An approach to correlate MS/MS data to amino acid sequences in a protein database. *J. Am. Soc. Mass Spectrom.* **1994**, *5*, 976–989.

(26) Carvalho, P. C.; Fischer, J. S.; Chen, E. I.; Yates, J. R., 3rd; Barbosa, V. C. PatternLab for proteomics: a tool for differential shotgun proteomics. *BMC Bioinf.* **2008**, *9*, 316.

(27) Carvalho, P. C.; Fischer, J. S.; Xu, T.; Yates, J. R., 3rd; Barbosa, V. C. PatternLab: from mass spectra to label-free differential shotgun proteomics. *Curr. Protoc. Bioinf.* **2012**, *13*, 13–19.

(28) Carvalho, P. C.; Yates, J. R., 3rd; Barbosa, V. C. Improving the TFC test for differential shotgun proteomics. *Bioinformatics* **2012**, *28* (12), 1652–1654.

(29) Liu, H.; Sadygov, R. G.; Yates, J. R., 3rd. A model for random sampling and estimation of relative protein abundance in shotgun proteomics. *Anal. Chem.* **2004**, *76* (14), 4193–4201.

(30) Conesa, A.; Götz, S.; García-Gómez, J. M.; Terol, J.; Talón, M.; Robles, M. Blast2GO: a universal tool for annotation, visualization and analysis in functional genomics research. *Bioinformatics* **2005**, *21* (18), 3674–3676.

(31) Ashburner, M.; Ball, C. A.; Blake, J. A.; Botstein, D.; Butler, H.; Cherry, J. M.; Davis, A. P.; Dolinski, K.; Dwight, S. S.; Eppig, J. T.; Harris, M. A.; Hill, D. P.; Issel-Tarver, L.; Kasarskis, A.; Lewis, S.; Matese, J. C.; Richardson, J. E.; Ringwald, M.; Rubin, G. M.; Sherlock, G. Gene ontology: tool for the unification of biology. The Gene Ontology Consortium. *Nat. Genet.* **2000**, *25* (1), 25–29.

(32) Emanuelsson, O.; Nielsen, H.; Brunak, S.; von Heijne, G. Predicting subcellular localization of proteins based on their N-terminal amino acid sequence. *J. Mol. Biol.* **2000**, *300*, 1005–1016.

(33) Horton, P.; Park, K.-J.; Obayashi, T.; Fujita, N.; Harada, H.; Adams-Collier, C. J.; Nakai, K. WoLF PSORT: protein localization predictor. *Nucleic Acids Res.* **2007**, *35*, W585–587.

(34) Petersen, T. N.; Brunak, S.; von Heijne, G.; Nielsen, H. SignalP 4.0: discriminating signal peptides from transmembrane regions. *Nat. Methods* **2011**, *8*, 785–786.

(35) Pierleoni, A.; Martelli, P. L.; Casadio, R. PredGPI: a GPI anchor predictor. *BMC Bioinf.* **2008**, *9*, 392.

(36) Cortázar, A. R.; Aransay, A. M.; Alfaro, M.; Oguiza, J. A.; Lavín, J. L. SECRETOOL: integrated secretome analysis tool for fungi. *Amino Acids* **2014**, *46* (2), 471–473.

(37) Fischer, S.; Brunk, B. P.; Chen, F.; Gao, X.; Harb, O. S.; Iodice, J. B.; Shanmugam, D.; Roos, D. S.; Stoeckert, C. J. Using OrthoMCL to assign proteins to OrthoMCL-DB groups or to cluster proteomes into new ortholog groups. *Curr. Prot. Bioinf.* **2011**, *35*, 6.12.1–6.12.19.

(38) Hooper, S. D.; Bork, P. Medusa: a simple tool for interaction graph analysis. *Bioinformatics* **2005**, *21* (24), 4432–4433.

(39) Shah, P.; Powell, A. L.; Orlando, R.; Bergmann, C.; Gutierrez-Sanchez, G. Proteomic analysis of ripening tomato fruit infected by *Botrytis cinerea*. *J. Proteome Res.* **2012**, *11* (4), 2178–2192.

(40) Rampitsch, C.; Day, J.; Subramaniam, R.; Walkowiak, S. Comparative secretome analysis of *Fusarium graminearum* and two of its non-pathogenic mutants upon deoxynivalenol induction in vitro. *Proteomics* **2013**, *13*, 1913–1921.

(41) Brown, N. A.; Antoniw, J.; Hammond-Kosack, K. E. The predicted secretome of the plant pathogenic fungus *Fusarium graminearum*: a refined comparative analysis. *PLoS One* **2012**, *7*, e33731.

(42) Shah, P.; Atwood, J. A.; Orlando, R.; El Mubarek, H.; Podila, G. K.; Davis, M. R. Comparative proteomic analysis of *Botrytis cinerea* secretome. *J. Proteome Res.* **2009**, *8* (3), 1123–1130.

(43) Manalil, N. S.; Junior Téó, V. S.; Braithwaite, K.; Brumley, S.; Samson, P.; Nevalainen, K. M. Comparative analysis of the *Metarhizium anisopliae* secretome in response to exposure to the greyback cane grub and grub cuticles. *Fungal Biol.* **2010**, *114* (8), 637–645.

(44) Freimoser, F. M.; Hu, G.; St Leger, R. J. Variation in gene expression patterns as the insect pathogen *Metarhizium anisopliae* adapts to different host cuticles or nutrient deprivation in vitro. *Microbiology* **2005**, *151* (2), 361–371.

(45) de Sousa Abreu, R.; Penalva, L. O.; Marcotte, E. M.; Vogel, C. Global signatures of protein and mRNA expression levels. *Mol. Biosyst.* **2009**, *5*, 1512–1526.

- (46) Maier, T.; Guell, M.; Serrano, L. Correlation of mRNA and protein in complex biological samples. *FEBS Lett.* **2009**, *583*, 3966–3973.
- (47) Schwanhäusser, B.; Busse, D.; Li, N.; Dittmar, G.; Schuchhardt, J.; Wolf, J.; Chen, W.; Selbach, M. Global quantification of mammalian gene expression control. *Nature* **2011**, *473* (7347), 337–342.
- (48) St Leger, R. J.; Wang, C. Genetic engineering of fungal biocontrol agents to achieve greater efficacy against insect pests. *Appl. Microbiol. Biotechnol.* **2010**, *85* (4), 901–907.
- (49) Schrimpf, S. P.; Weiss, M.; Reiter, L.; Ahrens, C. H.; Jovanovic, M.; Malmström, J.; Brunner, E.; Mohanty, S.; Lercher, M. J.; Hunziker, P. E.; Aebersold, R.; von Mering, C.; Hengartner, M. O. Comparative functional analysis of the *Caenorhabditis elegans* and *Drosophila melanogaster* proteomes. *PLoS Biol.* **2009**, *7* (3), e48.
- (50) Santi, L.; Silva, W. O. B.; Pinto, A. F.; Schrank, A.; Vainstein, M. H. Differential immunoproteomics enables identification of *Metarhizium anisopliae* proteins related to *Rhipicephalus microplus* infection. *Res. Microbiol.* **2009**, *160*, 824–828.
- (51) Su, Y.; Guo, Q.; Tu, J.; Li, X.; Meng, L.; Cao, L.; Dong, D.; Qiu, J.; Guan, X. Proteins differentially expressed in conidia and mycelia of the entomopathogenic fungus *Metarhizium anisopliae* sensu stricto. *Can. J. Microbiol.* **2013**, *59*, 443–448.
- (52) Manalil, N. S.; Junior Téo, V. S.; Braithwaite, K.; Brumley, S.; Samson, P.; Nevalainen, K. M. A proteomic view into infection of greyback canegrubs (*Dermolepida albohirtum*) by *Metarhizium anisopliae*. *Curr. Genet.* **2009**, *55* (5), 571–581.
- (53) Murad, A. M.; Noronha, E. F.; Miller, R. N. G.; Costa, F. T.; Pereira, C. D.; Mehta, A.; Caldas, R. A.; Franco, O. L. Proteomic analysis of *Metarhizium anisopliae* secretion in the presence of the insect pest *Callosobruchus maculatus*. *Microbiology* **2008**, *154*, 3766–3774.
- (54) Barros, B. H. R.; Silva, S. H.; Marques, E. R.; Rosa, J. C.; Yatsuda, P. A.; Roberts, D. W.; Braga, G. U. L. A proteomic approach to identifying proteins differentially expressed in conidia and mycelium of the entomopathogenic fungus *Metarhizium anisopliae*. *Fungal Biol.* **2010**, *114* (7), 572–579.
- (55) Bye, N. J.; Charnley, A. K. Regulation of cuticle-degrading subtilisin proteases from the entomopathogenic fungi, *Lecanicillium* spp: implications for host specificity. *Arch. Microbiol.* **2008**, *189* (1), 81–92.
- (56) Okino, N.; Ito, M. Ceramidase enhances phospholipase C-induced hemolysis by *Pseudomonas aeruginosa*. *J. Biol. Chem.* **2007**, *282* (9), 6021–6030.
- (57) Wang, C.; St Leger, R. J. Developmental and transcriptional responses to host and nonhost cuticles by the specific locust pathogen *Metarhizium anisopliae* var. *acridum*. *Eukaryotic Cell* **2005**, *4* (5), 937–947.
- (58) Bagga, S.; Hu, G.; Screen, S. E.; St Leger, R. J. Reconstructing the diversification of subtilisins in the pathogenic fungus *Metarhizium anisopliae*. *Gene* **2004**, *324*, 159–69.
- (59) Gry, M.; Rimini, R.; Stromberg, S.; Asplund, A.; Pontén, F.; Uhlén, M.; Nilsson, P. Correlations between RNA and protein expression profiles in 23 human cell lines. *BMC Genomics* **2009**, *10*, 365.
- (60) Dou, D.; Zhou, J. M. Phytopathogen effectors subverting host immunity: different foes, similar battleground. *Cell Host Microbe* **2012**, *12* (4), 484–495.
- (61) Tudzynski, P.; Heller, J.; Siegmund, U. Reactive oxygen species generation in fungal development and pathogenesis. *Curr. Opin. Microbiol.* **2012**, *15* (6), 653–659.
- (62) Heyno, E.; Alkan, N.; Fluhr, R. A dual role for plant quinone reductases in host-fungus interaction. *Physiol. Plant.* **2013**, *149*, 340–353.
- (63) Shang, Y.; Duan, Z.; Huang, W.; Gao, Q.; Wang, C. Improving UV resistance and virulence of *Beauveria bassiana* by genetic engineering with an exogenous tyrosinase gene. *J. Invertebr. Pathol.* **2012**, *109* (1), 105–109.
- (64) Wang, Z. L.; Zhang, L. B.; Ying, S. H.; Feng, M. G. Catalases play differentiated roles in the adaptation of a fungal entomopathogen to environmental stresses. *Environ. Microbiol.* **2013**, *15* (2), 409–418.
- (65) Xie, X. Q.; Li, F.; Ying, S. H.; Feng, M. G. Additive contributions of two manganese-cored superoxide dismutases (MnSODs) to antioxidation, UV tolerance and virulence of *Beauveria bassiana*. *PLoS One* **2012**, *7* (1), e30298.
- (66) Heller, J.; Tudzynski, P. Reactive oxygen species in phytopathogenic fungi: signaling, development, and disease. *Ann. Rev. Phytopathol.* **2011**, *49*, 369–390.
- (67) Baltoumas, F. A.; Theodoropoulou, M. C.; Hamodrakas, S. J. Interactions of the  $\alpha$ -subunits of heterotrimeric G-proteins with GPCRs, effectors and RGS proteins: a critical review and analysis of interacting surfaces, conformational shifts, structural diversity and electrostatic potentials. *J. Struct. Biol.* **2013**, *182* (3), 209–218.
- (68) Carneiro-Leão, M. P.; Andreote, F. D.; Araújo, W. L.; Oliveira, N. T. Differential expression of genes involved in entomopathogenicity of the fungi *Metarhizium anisopliae* var. *anisopliae* and *M. anisopliae* var. *acridum* (Clavicipitaceae). *GMR, Genet. Mol. Res.* **2011**, *10* (2), 769–778.
- (69) He, Y.; Xu, J.; Yu, Z. H.; Gunawan, A. M.; Wu, L.; Wang, L.; Zhang, Z. Y. Discovery and evaluation of novel inhibitors of mycobacterium protein tyrosine phosphatase B from the 6-Hydroxy-benzofuran-5-carboxylic acid scaffold. *J. Med. Chem.* **2013**, *56* (3), 832–842.
- (70) Li, Z.; Wang, C.; Xia, Y. Isolation of two Locust protein targets of a protein tyrosine phosphatase from *Metarhizium anisopliae* strain CQMa102. *J. Invertebr. Pathol.* **2008**, *99* (2), 151–155.
- (71) Wawra, S.; Belmonte, R.; Lobach, L.; Saraiva, M.; Willems, A.; van West, P. Secretion, delivery and function of oomycete effector proteins. *Curr. Opin Microbiol.* **2012**, *15* (6), 685–691.
- (72) Donofrio, N. M.; Raman, V. Roles and delivery mechanisms of fungal effectors during infection development: common threads and new directions. *Curr. Opin Microbiol.* **2012**, *15* (6), 692–698.
- (73) Déon, M.; Bourré, Y.; Gimenez, S.; Berger, A.; Bieysse, D.; de Lamotte, F.; Poncet, J.; Roussel, V.; Bonnot, F.; Oliver, G.; Framchel, J.; Seguin, M.; Leroy, T.; Roeckel-Drevet, P.; Pujade-Renaud, V. Characterization of a cassiicolin-encoding gene from *Corynespora cassiicola*, pathogen of rubber tree (*Hevea brasiliensis*). *Plant Sci.* **2012**, *185–186*, 227–237.
- (74) Morais do Amaral, A.; Antoniwi, J.; Rudd, J. J.; Hammond-Kosack, K. E. Defining the predicted protein secretome of the fungal wheat leaf pathogen *Mycosphaerella graminicola*. *PLoS One* **2012**, *7* (12), e49904.